CONF-781033--46

LBL-8135

MASTER

ENERGY-DEPENDENT LOSSES IN
PULSED-FEEDBACK PREAMPLIFIERS

Donald A. Landis, Norman W. Madden, and Fred S. Goulding

November 1978

ENERGY-DEPENDENT LOSSES IN
PULSED-FEEDBACK PREAMPLIFIERS

Donald A. Landis, Norman W. Madden, Fred S. Goulding

Lawrence Berkeley Laboratory
University of California
Berkeley, California 94720 U.S.A.

Preamplifier Design

Figure 1 shows a block diagram of a conventional pulsed-light feedback preamplifier. When the output voltage of the preamplifier exceeds a positive predetermined level, the charge restoration circuit is promptly activated. This is accomplished by turning on the LED that is optically coupled to the FET. The light from the LED (D) causes the drain to gate current to increases to a value (approximately 0.1-1 µA) many orders of magnitude greater than the detector leakage. This causes the preamplifier output to go in a negative direction. When the output voltage exceeds a predetermined lower level the LED is turned off. This reset time is in the range of 1 to 10 µs.

The loss of pulses activating the reset is easily calculated. If the range of the preamplifier output during reset is 2 V, and each detector pulse produces a 0.2 V step, and if we neglect the effect of detector leakage current, it requires ten pulses to activate a reset. The tenth pulse would be lost thereby producing 10% losses. If the detector pulses were only 20 mV, a 1% loss would result.

A block diagram of a pulsed-light feedback preamplifier which overcomes this problem is shown in Fig. 2. The reset circuit has two discriminators. The fixed threshold discriminator has a +2 V threshold and 4 V of hysteresis. If the preamplifier output voltage exceeds +2 V, then the LED is turned on and the output voltage rapidly goes in a negative direction until it reaches -2 V. The LED is then turned off. The other discriminator has a threshold that can be varied from 0 V to about 1.8 V. The setting of this threshold is dependent on the maximum energy to be measured by the spectrometer. When this discriminator fires a "Wait" one shot is triggered, and at the end of the "Wait" time, the fixed threshold discriminator is triggered. The "Wait" time is made longer than the time required to process the event in the main ampli-fier. The "Wait" time can be terminated early by a signal from the main amplifier just after the end of the signal processing time.

A schematic diagram of the new preamplifier is shown in Fig. 3. The preamplifier is built on two boards. The linear board contains a single charge-sensitive loop with a bipolar output. The front-end electronics, consisting of the detector, feedback capacitor, LED, FET, and FET heater are in the cryostat cooled nearly to liquid-nitrogen temperature. This stage has been designed to have a faster rise time than the usual pulsed-light feedback

preamplifiers used in x-ray spectrometers. It is used at shorter main amplifier peaking times and also in systems where fast timing information is required. The faster rise time is obtained by using low collector capacitance transistors and bootstrapping these capacitances where needed. The preamplifier has better than 5 ns rise time when using a TIS75 FET at the input with a 0.5 pF feedback capacitor and a detector of 15 pF capacitance. The output swing is limited to ±2 V by the discriminator on the logic board. The output transistors are protected against excessive current in case the output exceeds ±2 V.

The logic board contains the two limit discriminators, the "Wait" one-shot, and LED driver. The LED driver can supply a positive or negative current to the LED depending on the kind of LED that is available. For some time we have used the TIL 205 type (Visible Red) LED without lenses.[8] This type was mounted in a coaxial header with the outside grounded in our FET-LED package. It required a negative current to turn on the LED. Since Texas Instruments no longer manufactures this device we currently use the Spectronics* SE 1450-2 (near I.R.) LED, and this device requires a positive current. The 555 circuit is used to flash an LED on the case of the preamplifier to visually indicate the reset rate.

Figure 4 shows a photograph of the detector, FET, LED, feedback capacitor, and FET heater assembly. Different types of FETs are used depending on the detector capacitance. The types used (from the smallest to the largest) are 2N4416, BF817, TIS75 (chips), and the SFB8558. All are manufactured by Texas Instruments. Care must be taken to avoid any charge storage or fluorescent effects following a reset or the rate performance will be degraded. We have observed that some LEDs show light emmission after the current is shut off and that some capacitors exhibit charge-storage effects. This is more critical for gamma-ray than x-ray spectrometers because the noise level is a much smaller percentage of the reset amplitude in high-energy systems, and after-effects of the reset are more prominent[9].

Experimental Results

The experimental results presented here are representative of a current
system but not the very best. The detector used was a high-purity planar
device, 1.25 cm thick and 3.8 cm in diameter. Its capacitance was 13 pF, and
the detector bias was 1500 V. The feedback capacitance was 0.5 pF. The FET
used in this system was a TIS75 chip mounted on a 2N4416 type header. The
main amplifier pile-up rejector and biased amplifier used in this work was our
standard 11X8481P-5 x-ray amplifier system used with pulsed-light feedback.
This version contains an improved base-line restorer of the wrap-around type.
The peaking time used for all measurements except for the electronic resolu-
tion was 4.5 µs, with the shaping circuit trimmed to have no under-shoot.
Measurements were made of the electronic resolution as a function of the
peaking time, of the gamma-ray resolution at low and high rates, of any
energy-dependent losses and also of the coincidence timing resolution.

(i) Electronic Energy Resolution

The electronic energy resolution was measured using an RMS voltmeter with
the amplifier gain normalized using the ^{241}Am 60 keV gamma-ray.[10]

Figure 5 shows two curves of the (FWHM energy resolution)^2 versus the
peaking time of the shaper in the main amplifier. The lower curve is the
electronic resolution of the spectrometer with the final germanium detector;
while the upper curve is the resolution when using a cooled lithium-drifted
silicon test detector having about the same capacitance as the germanium
detector. This test is performed to make sure that the final germanium system
exhibits no additional noise due to series resistance or other potential noise
sources in the detector. The 20% reduction in resolution shown in the german-
ium detector curve (due to the lower average energy per hole-electron pair)
indicates that no additional noise sources are present. The general shape of
these curves (eV^2 proportional to $1/\tau$) shows the advantage of pulsed-light
feedback in preventing additional low frequency noise due to the charge
restoration system. This system is capable of obtaining a resolution of
500 eV at very low energies.

(ii) High-Rate Performance

The values in T_ble 1 illustrate the rate performance of the spectrometer for two different gamma-ray energies (^{57}Co and ^{60}Co), at low rates, and at 100 K counts per second.

TABLE 1

	LOW RATE-5 kc/s			HIGH RATE-100 kc/s	
SOURCE	FWHM keV	FWTM keV		FWHM keV	FWTM keV
^{57}Co 122 keV	0.836	1.55		0.836	1.55
^{60}Co 1.17 MeV	1.80	3.63		1.80	3.71

We observed no change in the measurment of the FWHM resolution (within the accuracy of the measurment (1-2%)) for count rates up to 100kc/s. The full-width at tenth maximum (FWTM) resolution did increase at the higher energy due to low-energy pulse pile-up. The resolution is worse than would be expected because the 848 amplifier contributes some noise at the short peaking times. We are developing a new amplifier with less input noise at high frequencies for use in high-energy spectrometers.

(iii) Energy-Dependent Dead-Time Losses

The preamplifier was fitted with a switch to permit operating the reset circuit with either delayed or prompt reset. Measurements were made using a pulse generator mixed with a gamma source at low rates and comparing the two operating modes. The input and output rates of the pulser counts were determined. As was expected, the delayed reset mode showed negligible losses compared to the prompt reset mode. A ^{13}C (γ,n) ^{16}O source producing 6.13 MeV gamma-rays was used to make the comparison at high energy. The most prominent peak at high energy was the double escape peak from the 6.13 MeV gamma-ray (at about 5.1 MeV). The prompt reset mode exhibited a loss of 25%

of the counts in the 5.1 MeV peak. This is compared with zero losses in the
delayed reset mode. This result was expected since the total ramp at the
preamplifier output corresponded to 20 MeV (i.e. four times the signal size).

(iv) Timing Resolution

The coincidence time resolution was measured using a ^{60}Co source. The
second timing input was derived from a 2" x 2" NE 213 liquid scintillator and
8575 photomultiplier tube. The preamplifier output was differentiated and
applied to a standard constant fraction discriminator with its threshold set
to 1 MeV. The PMT anode was connected to another CFD with its threshold also
set to 1 MeV. The relative timing was measured using a standard TAC and PHA.
The FWHM of the timing resolution curve was 0.8 ns.

Conclusions

The pulsed-light reset preamplifier described in the paper gives excellent
resolution at high rates without introducing the energy dependent losses
associated with the loss of pulses that trigger the reset in a conventional
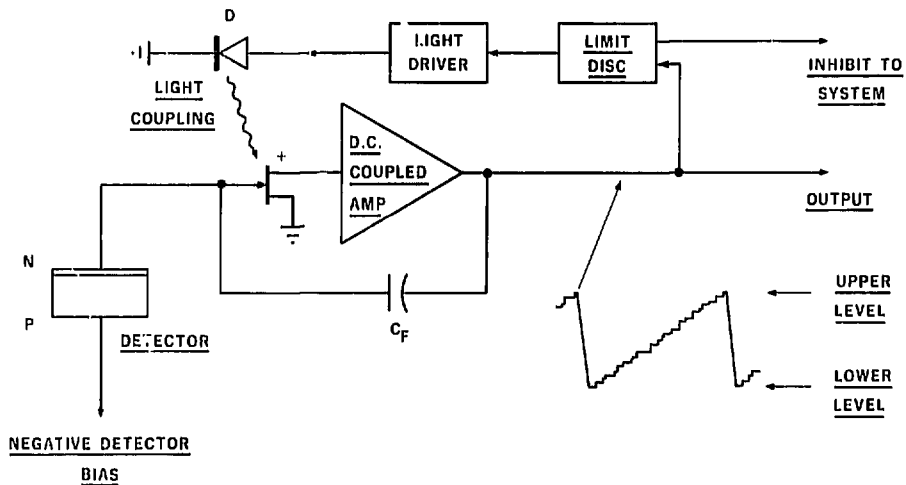pulsed-light reset preamplifier.

Acknowledgements

We wish to thank R. Cordi, A. Jue, D. Malone and E. Shaw for fabricating
the detector, mechanical parts and electronics used in this work, and M. Maier
for assisting us with some of the measurements.

References

1. V. Radeka, "State of the Art of Low Noise Amplifiers for Semiconductor
    Radiation Detectors", Proc. of the International Symposium on Nuclear
    Electronics, Versailles, Vol I pp 46/1-28,1969.

2. F. S. Goulding, J. Walton and D. F. Malone, "An Opto-Electronic Feedback
    Preamplifier for High-Resolution Nuclear Spectroscopy", Nucl. Instr. and
    Methods, 71, 273-279, 1969.

3. E. Elad, "Drain Feedback-A Novel Feedback Technique for Low-Noise
    Cryogenic Preamplifiers", IEEE Trans. Nucl. Sci., NS-19, No. 1, pg. 403,
    Feb. 1972

4. R. Kurz, "Low-Noise Preamplifier for High Count Rates". Internal report
    from Zentrallabor Fur Elektronik, Kernforschungsanlage Julich, Germany.

5. K. Kandiah and A. Stirling, Semiconductor Nuclear Particle Detectors and
    Circuits, National Academy of Science Publication 1593, Washington, D. C.,
    pg. 495, 1969.

6. V. Radeka, "Charge Amplification Without Charger Leak Resistor", IEEE
    Trans. Nucl. Sci., NS-17, No. 3, pg. 433, June, 1970.

7. D. A. Landis, F. S. Goulding, R. H. Pehl and J. T. Walton, "Pulsed
    Feedback Techniques for Semiconductor Detector Radiation Spectrometers",
    IEEE Trans. Nucl. Sci., NS-18, No. 1, pg. 115, Feb1971.

8. F. S. Goulding, J. T. Walton and R. H. Pehl, "Recent Results On The
    Optoelectronic Feedback Preamplifier", IEEE Trans. Nucl. Sci., NS-17,
    No. 1, pg. 220, Feb. 1970.

9. F. S. Goulding and D. A. Landis, "Some Electronic Aspects of Energy
    Measurements with Solid State Detectors", IEEE Trans. Nucl. Sci., NS-25,
    No. 2, pg. 898, April 1978.

10. "IEEE Standard Test Procedures for Amplifiers and Preamplifiers for
    Semiconductor Radiation Detec- tors for Ionizing Radiation", IEEE Std.
    301, 1976.

XBL 723-534

Fig. 1. Block diagram of a conventional
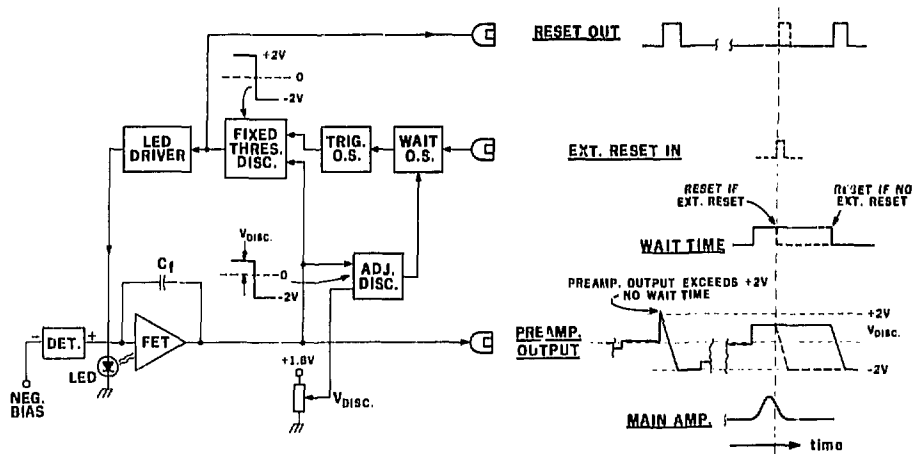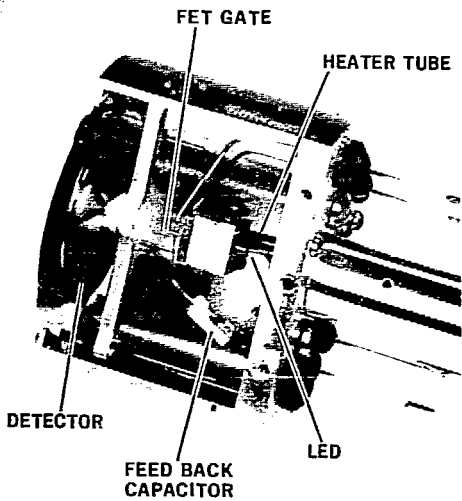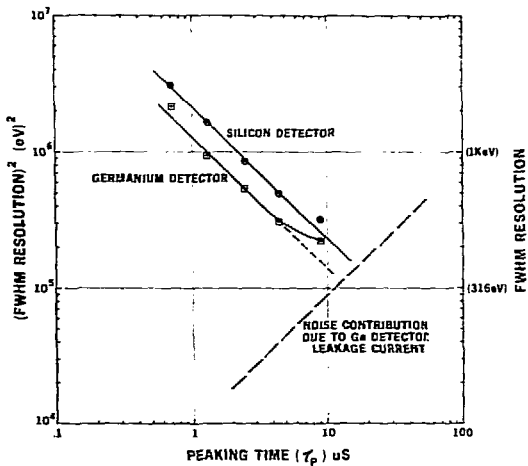pulsed-light reset preamplifier.

XBL · 10618

Fig. 2. Block diagram of a pulsed-light reset preamplifier
with no energy-dependent dead time losses.

Fig. 3.   Schematic diagram of new high-energy pulsed-light
          reset preamplifier.

CBB 779-8808A

Fig. 4. Photograph of crystal chamber containing
         the detector and FET-LED assembly.

XBL 789-11173 A

Fig. 5. Plot of (energy resolution)^2 versus
the peaking time of main amplifier
shaping time.